https://doi.org/10.5194/gmd-2023-126
Preprint. Discussion started: 27 June 2023

Geoscientific Model Development Discussions

The CO_2 and non-CO_2 climate effects of individual flights: simplified estimation of CO_2 equivalent emission factors

Robin N. Thor[1], Malte Niklaß[2], Katrin Dahlmann[1], Florian Linke[2], Volker Grewe[1, 3], and Sigrun Matthes[1]

[1]Deutsches Zentrum für Luft- und Raumfahrt (DLR), Institut für Physik der Atmosphäre, Oberpfaffenhofen, Germany
[2]Deutsches Zentrum für Luft- und Raumfahrt (DLR), Institut für Luftverkehr, Hamburg, Germany
[3]Faculty of Aerospace Engineering, Section Aircraft Noise and Climate Effects, Delft University of Technology, Delft, The Netherlands

Correspondence: Robin N. Thor (robin.thor@dlr.de)

Abstract. As aviation's contribution to anthropogenic climate change is increasing, industry aims at reducing the aviation climate effect. However, the large contribution of non-CO_2 effects to the total climate effect of aviation and their large variability for each individual flight inhibit finding appropriate guidance. Here, we present a method for the simplified calculation of CO_2 equivalent emissions, expressed using the physical climate metrics ATR100 or AGWP100, from CO_2 and non-CO_2 effects for a given flight, exclusively based on the aircraft seat category as well as the origin and destination airports. The simplified calculation method estimates non-CO_2 climate effects of air traffic as precisely as possible, without detailed information on the actual flight route, actual fuel burn, and current weather situation. For this purpose, we evaluate a global data set containing detailed flight trajectories, flight emissions, and climate responses, and derive a set of regression formulas for climate effects, which we call climate effect functions, as well as regression formulas for fuel consumption and NO_x emissions. Compared to previous studies, this method is available for a larger number of aircraft types, including most commercial airliners with seat capacities starting from 101 passengers, and delivers more specific results through a clustering approach. The climate effects calculated using the climate effect functions derived in this study exhibit a mean absolute relative error of 15.0 % and a root mean square error of 1.24 nK with respect to results from the climate response model AirClim. The climate effect functions are designed for climate footprint assessments, but would not create an incentive in an emission trading system, for which detailed information on the current weather as well as the actual flight route and profile would be required.

1 Introduction

Global aviation more than doubled from 2006 to 2019 in terms of revenue passenger kilometers (ICAO, 2015, 2021). The associated CO_2 emissions grew by 40% to 1036 $\mathrm{Tg(CO_2)yr^{-1}}$ during this time span (IEA, 2022). The COVID-19 crisis significantly reduced air transportation, with the worldwide amount of traffic plunging to 25% of the pre-COVID year 2019 in April 2020, and recovering to around 85% in 2022, based on an analysis of Flightradar24 data (Dube, 2023). As aviation is one of the fastest growing sectors, the share in global CO_2 emissions could rise from currently about 2 up to even 22% in 2050 (Cames et al., 2015). Apart from CO_2 emissions, also non-CO_2 emissions contribute to aviation-induced climate

https://doi.org/10.5194/gmd-2023-126
Preprint. Discussion started: 27 June 2023

Geoscientific Model Development Discussions

change. Especially the effects of contrail cirrus and NO_x emissions on the concentration of ozone increase the climate effect of aviation. Non-CO_2 effects were responsible for about two thirds of the total effective radiative forcing (ERF) in 2018 when considering all aviation emissions from 1940 to 2018 (Lee et al., 2021). The COVID-19 crisis reduced the overall climate impact of aviation, however, a significant reduction only occurs if it leads to changes in travel behavior (Grewe et al., 2021).

In this context, it is very important to reduce the climate effect of aviation. There are different mitigation options allowing to achieve this goal. Beside reducing the number of flights, e.g. by replacing in-person by virtual meetings, the climate effect can be reduced by alternative fuels and technical or operational measures. Technical measures include the reduction of the specific fuel consumption through reduced airframe weight, optimized aerodynamics, and engine performance. In addition, optimized aircraft design for flying in lower altitudes or in a wider range of altitudes could mitigate the downsides of climate-optimized flying (e.g., Dahlmann et al., 2016b). The climate effect can also be reduced by using alternative fuels like sustainable aviation fuel (SAF) or liquid hydrogen. These fuels are potentially CO_2-neutral if the fuel is produced with renewable energy. However, the replacement of conventional fuels by SAF or liquid hydrogen also affects non-CO_2 effects, e.g. contrails (Voigt et al., 2021; Brazzola et al., 2022; Dray et al., 2022). Efficient flight guidance can reduce the fuel consumption and the effect on climate. As the climate effect of a flight depends not only on the emission strength, but also on the emission location and the time of emission, it is possible to reduce the climate effect if climate-sensitive regions are avoided by these so-called climate-optimized flights (Grewe et al., 2017b; Niklaß et al., 2019b; Matthes et al., 2021). The mitigation of non-CO_2 climate effects often comes along with an increase in cash operating costs. Therefore, the inclusion of non-CO_2 effects in emission trading schemes or marked based measures as incentives for reducing non-CO_2 climate effects could be a significant contribution to the agreed climate goals of Paris (Grewe et al., 2021).

Carbon dioxide equivalents ($CO_{2,e}$) are a common metric for unitizing the climate effects of various climate agents. Since the climate effect of CO_2 is fairly well understood due to its independence of emission source and location, it is reasonable to express non-CO_2 effects in relation to the effects of emitting a certain amount of CO_2. For a given type and amount of a climate agent i, resulting $CO_{2,e}$ cause the same climate response, e.g. radiative forcing (RF) or ΔT, over a specific time horizon (e.g. 20, 50 or 100 years) as CO_2:

$$CO_{2,e,\text{total}} = CO_2 + \sum_i CO_{2,e,i} \tag{1}$$

In principle, there are several $CO_{2,e}$ calculation methods available that are designed for different applications. In the context of aviation, the simplest options for the computation of $CO_{2,e}$ are constant $CO_{2,e}$ factors, such as the Radiative Forcing Index (RFI, IPCC, 1999), followed by $CO_{2,e}$ factors that depend on the flight distance of the evaluated flight. However, Forster et al. (2006) clearly pointed at the limiting shortcomings of the RFI concept, such as a large variation with time for constant emissions, and concluded that RFI is inappropriate for comparing emissions. In addition, the altitude dependency of non-CO_2 effects has to be considered in the $CO_{2,e}$ calculation method to avoid misguiding incentives (Faber et al., 2008; Scheelhaase et al., 2016; Niklaß et al., 2019a). This requires detailed information about the flown aircraft trajectory (altitude profile) of each flight. However, to obtain the flown altitude profile, one needs to query the flight data, which is an elaborate process. Instead, here, we use much simpler $CO_{2,e}$ calculation methods for the climate footprint assessment of single flights. The accuracy of

https://doi.org/10.5194/gmd-2023-126
Preprint. Discussion started: 27 June 2023

Geoscientific Model Development Discussions

these simple factors was investigated, for example, by Dahlmann et al. (2023), who analyzed the climate effect of one typical long-haul aircraft type of A330-200 aircraft for more than 1000 international city pairs using the climate response model AirClim (Grewe and Stenke, 2008; Dahlmann et al., 2016a). They found an increase in $CO_{2,e}$ factors with flight distances as these typically correlate with an increased average flight altitude for distances shorter than 4000 km. This increase in total $CO_{2,e}$ values becomes less significant for flight distances longer than 4000 km, as average flight altitude hardly changes on long-haul flights. Dahlmann et al. (2023) then fitted altitude and latitude dependent regression formulas to the AirClim results, which can be used for a simplified estimation of aviation climate effects. They found that these regression formulas can be used to represent the aviation climate effects much better than a constant factor. While the root mean square error for a constant factor of 3.4 was about 1.18, that obtained with the regression formulas was about 0.24, with 95% of the estimates lying within a $\pm 20\%$ range.

Here, we expand the study by Dahlmann et al. (2023) and develop a simplified estimation method for aircraft climate effects, expressed using the average temperature response over 100 years (ATR100) as a climate metric, using climate effect functions that are valid for all passenger aircraft with a seat capacity of over 100. While Dahlmann et al. (2023) only analyzed one aircraft type, we here analyze the climate impact for different aircraft types. An additional difference to Dahlmann et al. (2023) is the different emission development. While Dahlmann et al. (2023) used constant emissions over a typical lifetime of an aircraft of 32 years, we here use increasing emissions over the next 100 years. In both studies, the effects of historical emissions are neglected. We consider the climate impacts of aircraft emissions of CO_2, NO_x, and H_2O as well as contrail-induced cloudiness, but ignore the effects of aerosol emissions through aerosol–radiation interactions and aerosol–cloud interactions. This simplified method provides a precise estimate of the non-CO_2 climate effects of air traffic without requiring detailed information on the actual flight route, the amount of emissions, and the current weather situation. Instead, it is only based on the seat capacity as well as the distance and latitude of the flight, two quantities that can be easily computed from the airport pair.

In the first step, we evaluate a data set containing a global set of detailed flight trajectories, flight emissions (Section 2.1), and climate responses (Section 2.2). After establishing three different clusters of flights using a K-means method (Section 2.3), we generate climate effect functions, which are regression formulas for the climate response (Section 2.4). We also derive regression formulas for fuel consumption and NO_x emissions (Section 2.5) that can be used as input for the climate effect functions. We then discuss the resulting simplified formulas for the climate effect of individual flights (Section 3). The resulting equations have been implemented into a simplified estimation tool, for which a user manual is available in Appendix A.

2 Method

2.1 Global emission inventories and climate responses of the DLR project WeCare

As a basis for the derivation of the climate effect functions that allow for the determination of CO_2 equivalent climate effects, data from the project WeCare (Utilizing WEather information for ClimAte efficient and ecoefficient futuRE aviation, Grewe et al., 2017a) was used, which was an internal project of the German Aerospace Center (Deutsches Zentrum für Luft-

https://doi.org/10.5194/gmd-2023-126
Preprint. Discussion started: 27 June 2023

und Raumfahrt; DLR). The project addressed both an improvement of the understanding of aviation-influenced atmospheric processes and an assessment of different mitigation options. An essential output of the project was a new set of emission inventories for global aviation (Grewe et al., 2017a). The network of flight trajectories was developed following a four-layer approach implemented in the AIRCAST method (Ghosh et al., 2016), starting from an origin–destination passenger demand network that was built up from exogenous socio-economic scenarios, via the passenger routes network (sequence of flight segments, a passenger actually travelled from origin to destination) to an aircraft movements network, which assigns aircraft categories to the resulting flight routes and provides flight frequency information. The final step is a simulation of trajectories based on the aircraft movements obtained from the aircraft movements network layer using the Global Air Traffic Emissions Distribution Laboratory (GRIDLAB) developed by DLR (Linke, 2016). Each mission, defined by departure and arrival cities, aircraft type, and load factor, was simulated under typical operational conditions, resulting in a network of flight trajectories. For this purpose, DLR's Trajectory Calculation Module (TCM; Lührs et al., 2014) was used that applies simplified equations of motion known as the Total Energy Model.

Based on the aircraft's engine state determined by parameters such as thrust and fuel flow, the engine emission distribution of NO_x, CO, and HC species along the trajectory was determined by applying the Boeing Fuel Flow Method 2 (DuBois and Paynter, 2006). The amount of CO_2 and H_2O emissions was calculated assuming a linear relationship to the fuel burn. The mapping of emission distributions of all flights onto a geographical grid resulted in 3D inventories. In WeCare, using the approach mentioned above, emission inventories and the corresponding climate effect were calculated for the years 2015 to 2050 in 5-year steps. The forecast was based on the reference year 2012. The resulting flight plan of the base year consisted of 47,057 airport pairs and approximately 31 million flights. As it was found that aircraft with more than 100 seats contribute to about 95% of the globally available seat kilometres (ASK), only aircraft with more than 100 seats were covered by the study to reduce complexity and ensure model availability. Therefore, five different aircraft size categories (based on the number of seats) were considered in the inventories (101-151 seats; 152-201 seats; 202-251 seats; 252-301 seats; 302-600 seats) and each size category was modelled using one representative aircraft type (plus one backup aircraft type). The representative aircraft type was selected such that it contributes to a significant share of the respective size category. Respective engine emission characteristics were taken from the Aircraft Engine Emissions Databank of the International Civil Aviation Organization (ICAO).

2.2 Computation of climate effects of single flights using AirClim

From the WeCare project, only aggregated flight and emission inventories were available. The determination of climate effect functions that can be applied to individual flights requires a disaggregation of the WeCare data set. Therefore, for the entire flight inventory from WeCare emission distributions were re-calculated on a per-flight basis following the method described above. The resulting single trajectory inventories were then processed with the non-linear climate response model AirClim (Grewe and Stenke, 2008; Dahlmann et al., 2016a), to obtain the climate effect per species for each flight in the flight plan.

AirClim combines aircraft emission data (longitude, latitude, and altitude) with a set of pre-calculated non-linear emission–response relations for a set of atmospheric locations to calculate the temporal development of the global near-surface temperature change. AirClim includes the impact of the climate agents CO_2, H_2O, CH_4, and O_3 (the latter two result from NO_x

https://doi.org/10.5194/gmd-2023-126
Preprint. Discussion started: 27 June 2023

Geoscientific Model Development Discussions

emissions), as well as contrail-induced cloudiness (CiC). For deriving the atmospheric responses for H_2O and NO_x-induced changes in O_3 and CH_4, 85 steady-state simulations for the year 2000 were performed with the DLR climate–chemistry model E39/CA, prescribing normalized emissions of NO_x and H_2O at various atmospheric regions (Fichter, 2009). For the impact of CiC, we use atmospheric and climate responses considering the local probability of fulfilling the Schmidt-Appleman criterion as well as ice-supersaturated regions, which were obtained from simulations with ECHAM4-CCMod (Burkhardt and Kärcher, 2011). We follow a climatological approach in the calculation of the climate impact, meaning that the calculated values for the climate impact represent a mean over all weather situations averaging over individual spatially and temporally resolved responses.

For analyzing the climate impact, we assume emissions starting in 2012 and a future increase in emissions according to the scenario Fa1 of the Intergovernmental Panel on Climate Change (IPCC, 1992), which is a reference scenario developed by the International Civil Aviation Organization Forecasting and Economic Support Group (ICAO FESG) with mid-range economic growth and technology for both improved fuel efficiency and NO_x reduction (IPCC, 1999). For background concentrations of CO_2 and CH_4, which influence the climate impact of CO_2 and CH_4 emissions, we assume IPCC scenario RCP4.5 (Meinshausen et al., 2011). We quantify the climate impact as the ATR100 (average temperature response), which is the mean near-surface temperature change over 100 years.

In the data structure for each of the 57631 flights, characterized by origin and destination airport as well as aircraft size category, the resulting amounts of engine emissions were stored together with the climate effect per species. This database was then used to derive the climate effect functions as well as regression formulas for fuel use and NO_x emissions.

2.3 Clustering of flights by climate effects using K-means

Next, we want to derive the climate effect functions, which are regression formulas for the total climate effect based on the climate effect components of the 57631 flights in the database due to emissions of CO_2, NO_x, and H_2O, as well as CiC, and which allow for a quick determination of the climate effect of a given flight. The analysis uses the following quantities: flight distance along a great circle, mean latitude along the great circle, fuel use, NO_x emissions, and climate effect. The climate effect is further divided into climate effects from individual components (CO_2, H_2O, CiC, O_3, PMO, CH_4).

Due to the large variety of importance of the different climate effect components among different flights, it is challenging to find a single set of equations that would reasonably predict the climate effect under most circumstances. Therefore, in the first step, we apply a K-Means clustering algorithm to separate the flights into several clusters. This clustering is based solely on the share of the six aforementioned components of the climate effect in the total climate effect:

$$\frac{\mathrm{ATR100}_{\mathrm{CO_2}}}{\mathrm{ATR100}_{\mathrm{tot}}}, \frac{\mathrm{ATR100}_{\mathrm{H_2O}}}{\mathrm{ATR100}_{\mathrm{tot}}}, \frac{\mathrm{ATR100}_{\mathrm{CiC}}}{\mathrm{ATR100}_{\mathrm{tot}}}, \frac{\mathrm{ATR100}_{\mathrm{O_3}}}{\mathrm{ATR100}_{\mathrm{tot}}}, \frac{\mathrm{ATR100}_{\mathrm{PMO}}}{\mathrm{ATR100}_{\mathrm{tot}}}, \frac{\mathrm{ATR100}_{\mathrm{CH_4}}}{\mathrm{ATR100}_{\mathrm{tot}}}$$

This ensures that flights in a given cluster have similar climate effect characteristics. The clustering is not directly dependent on proxy quantities to the climate effect, such as the amount and location of the emissions. We use an implementation by the

https://doi.org/10.5194/gmd-2023-126
Preprint. Discussion started: 27 June 2023

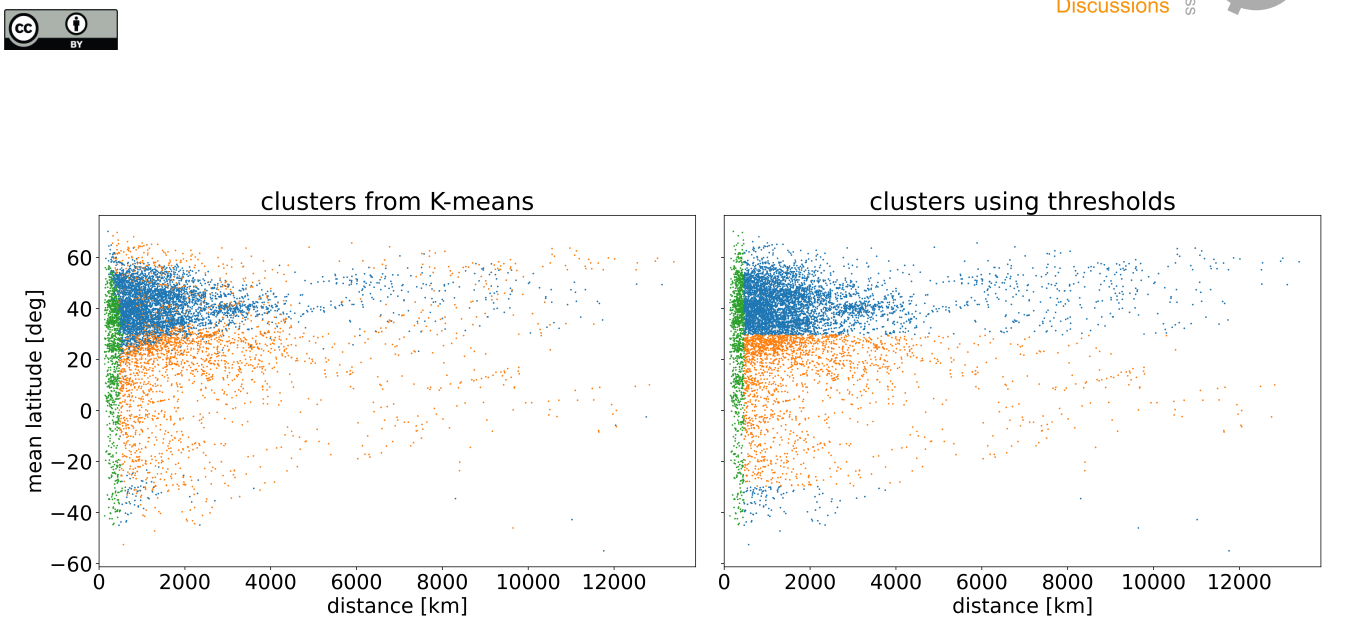

Figure 1. Clustering of flights, as obtained by the K-Means clustering algorithm (left) and as delineated by simple thresholds (right), shown in the latitude–distance space. Each color corresponds to one cluster. We name them the short-flight cluster (green), the tropical cluster (orange), and the mid-latitude cluster (blue).

free software machine learning library for the Python programming language scikit-learn (Pedregosa et al., 2011) and scale the input quantities to the standard normal distribution before clustering. We find a partition into three clusters to be most useful, as larger numbers of clusters lead to some clusters, whose distinctions do not have a clear physical interpretation. The resulting three clusters occupy distinct areas in the latitude-distance space (Fig. 1). We therefore name them the short-flight cluster (green), the tropical cluster (orange), and the mid-latitude cluster (blue).

In the second step, simple thresholds are derived which separate the flights into three categories that approximate the found clusters. This is necessary to be able to categorize also new flights that are not contained in the data set used for this analysis. One threshold is a maximum distance for the short-flight cluster, and another threshold is the absolute mean latitude confining the tropical cluster. We choose the values for these thresholds in such a way that the amount of wrongly categorized flights is minimized. This leads to a threshold distance of 462.5 km below which flights are categorized as belonging to the short-flight cluster, and a threshold mean latitude of $\pm 29.7°$ within which flights are categorized as belonging to the tropical cluster. All other flights are categorized into the mid-latitude cluster. This approximation wrongly categorizes 16.8% of flights (5859 flights). The resulting simplified clustering is shown in Fig. 1.

The three clusters have distinct characteristics (Fig. 2). The short-flight cluster has a negligible contribution of contrails to the climate effect at an average of 3.5% of the total climate effect, and a strong contribution of CO_2 at an average of 57.4% of the total climate effect. Flights in this cluster are very short and therefore often do not reach the required altitude of at least about $8\mathrm{km}$ (e.g.; Kärcher, 2018) for contrail formation. The climate effect of the tropical cluster is dominated by contrails (average contribution of 56.6%) because strong contrail formation occurs at tropical latitudes. The mid-latitude cluster contains the remaining flights and has large climate effect contributions from NO_x and H_2O (average contributions of 49.1% and 6.8%, respectively; see below for further discussion).

https://doi.org/10.5194/gmd-2023-126
Preprint. Discussion started: 27 June 2023

Geoscientific Model Development Discussions
Open Access
EGU

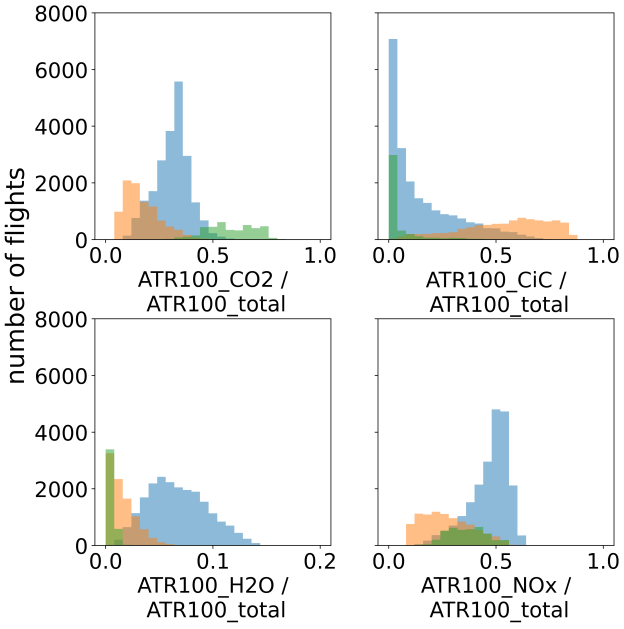

Figure 2. Histograms of the share of each climate effect component in the total climate effect for each cluster.

2.4 Derivation of climate effect functions

For each of the simplified clusters, a climate effect function is derived which approximates the climate effect for a given flight. Figures 3-5 show the climate effect of each flight as functions of the flight distance and the mean latitude. Emissions of NO_x in the southern hemisphere have a stronger climate effect than those in the northern hemisphere (Fig. 4b; 5b) due to the lower background concentrations in that region (Köhler et al., 2013). The climate effect of H_2O is largest when it is emitted in the lowermost stratosphere. Therefore, its climate effect is low in the tropics (Fig. 5e), where the tropopause lies above cruise altitude, as well as for short flights at any latitude (Fig. 3d), which do not reach a sufficient flight altitude to emit into the stratosphere. Similarly, very short flights often do not reach the required altitude for contrail formation (Fig. 3g). The contrail–cirrus climate effect is largest for flights in the tropics (Fig. 5h) due to the increased radiation. The usage of clusters enables us to find climate effect functions that follow these trends in the data more closely. Following Dahlmann et al. (2023), the climate effect obeys the pattern

$$\begin{aligned} \mathrm{ATR100_{tot}} = &\quad \mathrm{ATR100_{CO_2}} + \mathrm{ATR100_{NO_x}} \\ &+ \mathrm{ATR100_{H_2O}} + \mathrm{ATR100_{CiC}} \\ = &\quad c_{\mathrm{CO_2}} f + c_{\mathrm{NO_x}}(d, \bar{\phi}) e \\ &+ c_{\mathrm{H_2O}}(d, \bar{\phi}) f + c_{\mathrm{CiC}}(d, \bar{\phi}) d, \end{aligned} \tag{2}$$

https://doi.org/10.5194/gmd-2023-126
Preprint. Discussion started: 27 June 2023

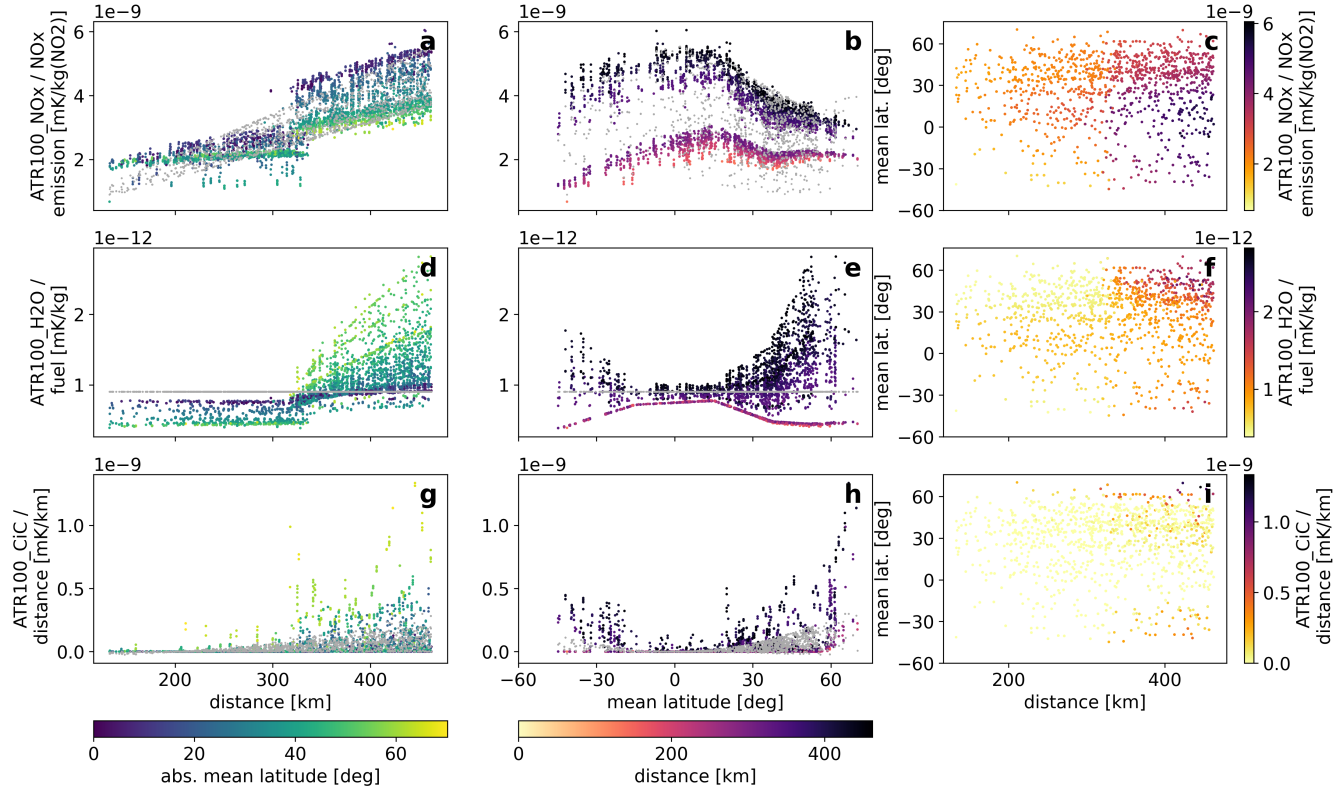

Figure 3. Climate metrics $\mathrm{ATR100}_{\mathrm{NO_x}}/e$ (top row), $\mathrm{ATR100}_{\mathrm{H_2O}}/f$ (middle row), $\mathrm{ATR100}_{\mathrm{CiC}}/d$ (bottom row) as a function of distance d (left column), mean latitude $\bar{\phi}$ (middle column), and both (right column) for the short-flight cluster. Colorful dots denote the values obtained from AirClim and gray dots are fit results from the climate effect function (Eq. 2).

where f is the fuel use, e are the $\mathrm{NO_x}$ emissions, d is the flown distance, $\bar{\phi}$ is the mean latitude, $c_{\mathrm{CO_2}}$, $c_{\mathrm{NO_x}}$, $c_{\mathrm{H_2O}}$, and c_{CiC} are cluster-dependent climate effect functions. These formulas are intended to fit the respective partial climate effects $\mathrm{ATR100}_{\mathrm{CO_2}}/f$, $\mathrm{ATR100}_{\mathrm{NO_x}}/e$, $\mathrm{ATR100}_{\mathrm{H_2O}}/f$, and $\mathrm{ATR100}_{\mathrm{CiC}}/d$, where $\mathrm{ATR100}_{\mathrm{NO_x}} = \mathrm{ATR100}_{\mathrm{O_3}} + \mathrm{ATR100}_{\mathrm{PMO}} + \mathrm{ATR100}_{\mathrm{CH_4}}$ is the combined climate effect of $\mathrm{NO_x}$ emissions. We do not directly fit the climate effects $\mathrm{ATR100}_{\mathrm{CO_2}}$, $\mathrm{ATR100}_{\mathrm{NO_x}}$, $\mathrm{ATR100}_{\mathrm{H_2O}}$, and $\mathrm{ATR100}_{\mathrm{CiC}}$ because they are linearly or almost linearly related to f, e, f, and c, respectively. Instead, we fit the partial cluster-dependent climate effect functions $c_{\mathrm{CO_2}}$, $c_{\mathrm{NO_x}}$, $c_{\mathrm{H_2O}}$, and c_{CiC}. The climate effect function for $\mathrm{CO_2}$ is fixed at $c_{\mathrm{CO_2}} = 8.145 \times 10^{-11}\mathrm{mKkg}^{-1}(\mathrm{fuel})$, because the climate effect of $\mathrm{CO_2}$ is independent of the emission location in AirClim, so that no fit is required.

https://doi.org/10.5194/gmd-2023-126
Preprint. Discussion started: 27 June 2023

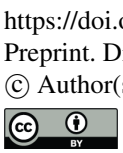

Geoscientific Model Development Discussions

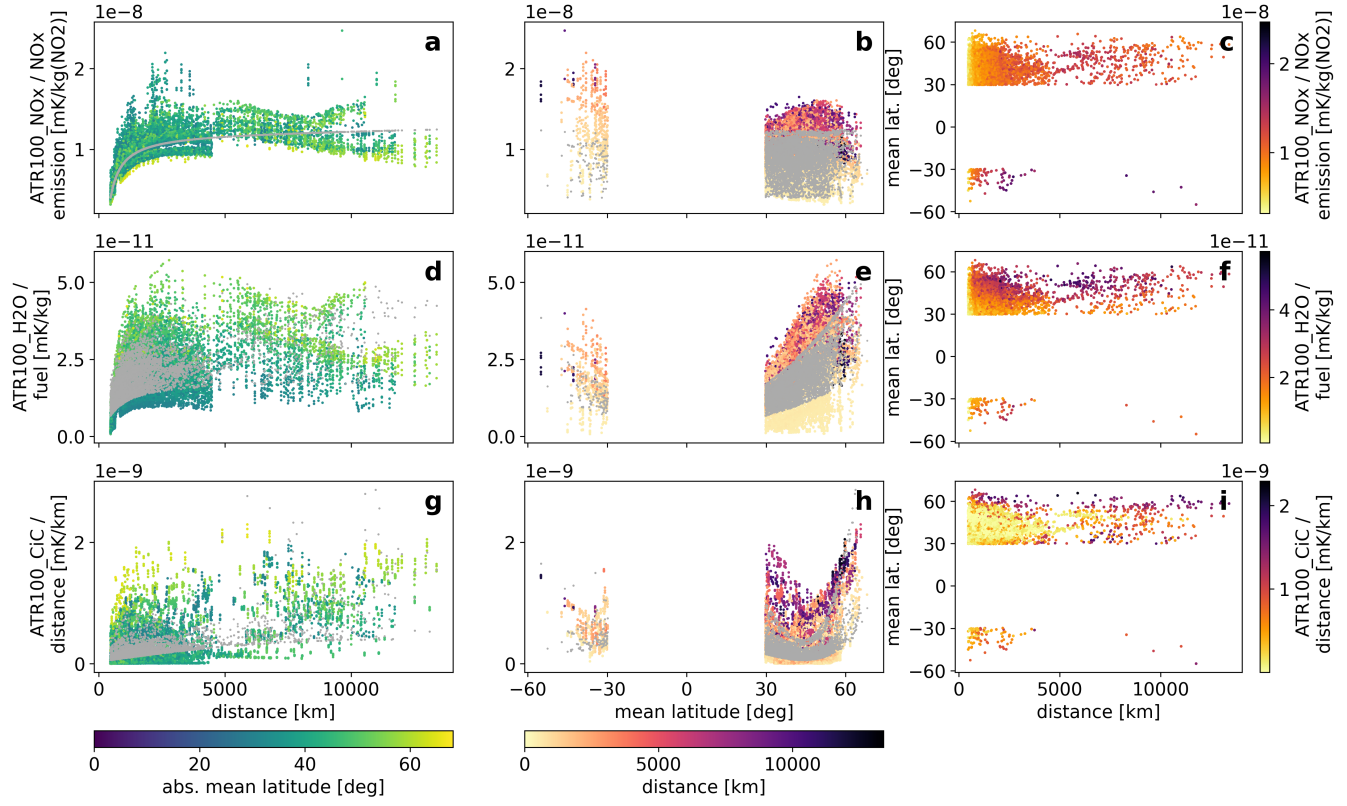

Figure 4. Same as Fig. 3, but for the mid-latitude cluster.

The partial cluster-dependent climate effect functions are chosen based on the behavior of the respective values in latitude–distance space (Fig. 3-5) as

$$
\begin{aligned}
c_{\mathrm{NO_x}} = \quad & \left(a_{\mathrm{NO_x,s},0} d + a_{\mathrm{NO_x,s},1}\right) \times \\
& \left(a_{\mathrm{NO_x,s},2} \bar{\phi}^4 + a_{\mathrm{NO_x,s},3} \bar{\phi}^3 + a_{\mathrm{NO_x,s},4} \bar{\phi}^2 \right. \\
& \left. + a_{\mathrm{NO_x,s},5} \bar{\phi} + a_{\mathrm{NO_x,s},6}\right) \qquad (3) \\
c_{\mathrm{H_2O}} = \quad & a_{\mathrm{H_2O,s},0} \\
c_{\mathrm{CiC}} = \quad & \left(a_{\mathrm{CiC,s},0} d^2 + a_{\mathrm{CiC,s},1} d + a_{\mathrm{CiC,s},2}\right) \bar{\phi}^2
\end{aligned}
$$

https://doi.org/10.5194/gmd-2023-126
Preprint. Discussion started: 27 June 2023

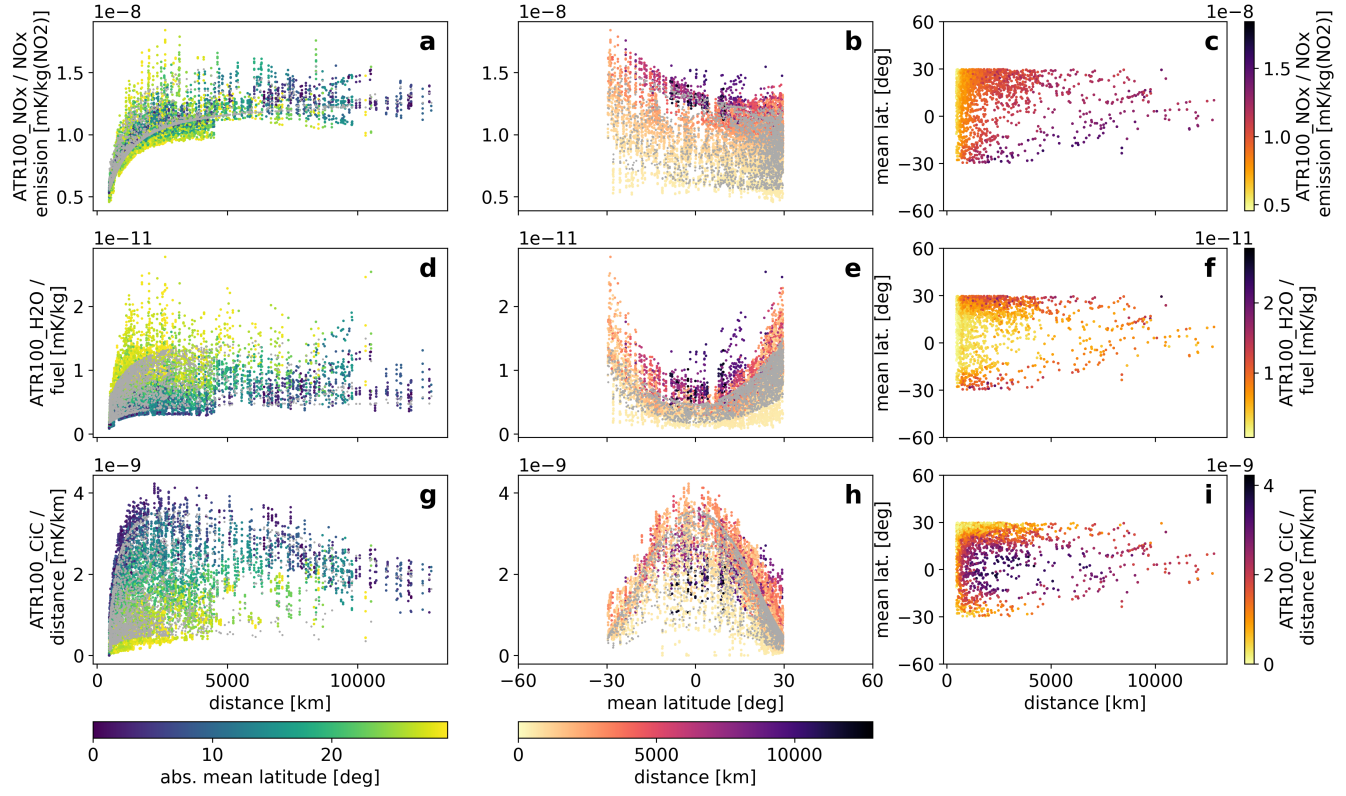

Figure 5. Same as Fig. 3, but for the tropical cluster.

for the short-flight cluster,

$$
\begin{aligned}
c_{\mathrm{NO_x}} = \; & a_{\mathrm{NO_x,m,0}} \arctan(a_{\mathrm{NO_x,m,1}} d) \\
& + a_{\mathrm{NO_x,m,2}} d + a_{\mathrm{NO_x,m,3}} \\
c_{\mathrm{H_2O}} = \; & a_{\mathrm{H_2O,m,0}} \arctan(a_{\mathrm{H_2O,m,1}} d) \times \\
& \left(a_{\mathrm{H_2O,m,2}} \bar{\phi}^2 + a_{\mathrm{H_2O,m,3}}\right) \\
c_{\mathrm{CiC}} = \; & \left(a_{\mathrm{CiC,m,0}} d^2 + a_{\mathrm{CiC,m,1}} d + a_{\mathrm{CiC,m,2}}\right) \times \\
& \left(a_{\mathrm{CiC,m,3}} \bar{\phi}^4 + a_{\mathrm{CiC,m,4}} \bar{\phi}^3 + a_{\mathrm{CiC,m,5}} \bar{\phi}^2\right. \\
& \left. + a_{\mathrm{CiC,m,6}} \bar{\phi} + a_{\mathrm{CiC,m,7}}\right)
\end{aligned}
\tag{4}
$$

https://doi.org/10.5194/gmd-2023-126
Preprint. Discussion started: 27 June 2023

Geoscientific Model Development Discussions

for the mid-latitude cluster, and

$$
\begin{aligned}
c_{\mathrm{NO_x}} = \quad & (a_{\mathrm{NO_x,t,0}} \arctan(a_{\mathrm{NO_x,t,1}} d) + a_{\mathrm{NO_x,t,2}}) \times \\
& \left(a_{\mathrm{NO_x,t,3}} \bar{\phi}^2 + a_{\mathrm{NO_x,t,4}} \bar{\phi} + a_{\mathrm{NO_x,t,5}}\right) \\
c_{\mathrm{H_2O}} = \quad & a_{\mathrm{H_2O,t,0}} \arctan(a_{\mathrm{H_2O,t,1}} d) \times \\
& \left(a_{\mathrm{H_2O,t,2}} \bar{\phi}^2 + a_{\mathrm{H_2O,t,3}}\right) \\
c_{\mathrm{CiC}} = \quad & (a_{\mathrm{CiC,t,0}} \arctan(a_{\mathrm{CiC,t,1}} d) \\
& + a_{\mathrm{CiC,t,2}} d + a_{\mathrm{CiC,t,3}}) \times \\
& \left(a_{\mathrm{CiC,t,4}} \bar{\phi}^4 + a_{\mathrm{CiC,t,5}} \bar{\phi}^2 + a_{\mathrm{CiC,t,6}}\right)
\end{aligned}
\tag{5}
$$

for the tropical cluster. The inputs for these climate effect functions are the flight distance d in km and the mean latitude $\bar{\phi}$ in degrees. The resulting climate effects are given in units of $\mathrm{mKkg^{-1}(NO_2)}$ for $c_{\mathrm{NO_x}}$, $\mathrm{mKkg^{-1}(fuel)}$ for $c_{\mathrm{H_2O}}$, and $\mathrm{mKkm^{-1}}$ for c_{CiC}, respectively. The climate effects, particularly those of $\mathrm{NO_x}$ and $\mathrm{H_2O}$, exhibit discontinuities at flight distances of $\sim$ 315 km and $\sim$ 4600 km, which are related to higher calculated flight levels for flights with longer distances. These discontinuities pose challenges on the fitting with continuous analytic functions. In the case of the $\mathrm{H_2O}$ climate effect for the short-flight cluster, we chose to use the mean instead of a more sophisticated formula, as the contribution of $\mathrm{H_2O}$ to the total climate effect is very low for short flights in any case. The latitudinal dependency of the climate effects is generally modelled with polynomials, where the number of terms depends on the complexity and symmetry of the data's behavior. The dependency of the climate effects on the flight distance is modelled using a combination of polynomial terms and arctangents, which capture the behavior of an initial steep increase in and later flattening of the climate effect data (see also Dahlmann et al., 2023). The coefficients a are determined for each of the nine regression formulas by a non-linear least-squares fit and are given in Table 1. The resulting $\mathrm{CO_{2,e}}$ factor can then be computed as

$$
\mathrm{CO_{2,e}} = \frac{\mathrm{ATR100_{tot}}}{\mathrm{ATR100_{CO_2}}} \,. \tag{6}
$$

2.5 Derivation of fuel and $\mathrm{NO_x}$ functions

Using a selection of all flights of a given seat category from the database of all flights, we derived regression formulas which approximate the burnt fuel (BF) and the emission index of $\mathrm{NO_x}$ ($\mathrm{EI(NO_x)}$) for a given flight distance d (Fig. 6). These regression formulas are based on fuel uses and $\mathrm{NO_x}$ emission indices derived from the Boeing and DLR fuel flow methods. Fuel functions obey the pattern

$$
\mathrm{BF} = a_0 + a_1 d + a_2 d^2 \,, \tag{7}
$$

with the coefficients a_i as given in Table 2. The coefficient of determination R^2 is > 0.99 for all seat categories.

https://doi.org/10.5194/gmd-2023-126
Preprint. Discussion started: 27 June 2023

Geoscientific Model Development Discussions
Open Access
EGU

Table 1. Best-fit solutions for the coefficients in Eq. 3-5. These coefficients are only valid when using the respective equations with flight distances d in km and mean latitudes $\bar{\phi}$ in degrees.

short-flight cluster			
i	$a_{\mathrm{NO_x,s,i}}$	$a_{\mathrm{H_2O,s,i}}$	$a_{\mathrm{CiC,s,i}}$
0	$2.00347786 \times 10^{-15}$	$9.03099431 \times 10^{-13}$	$4.56196374 \times 10^{-19}$
1	$-7.13997187 \times 10^{-14}$	–	$-1.95682151 \times 10^{-17}$
2	2.365071×10^{-4}	–	$-1.4614218 \times 10^{-14}$
3	$1.54249099 \times 10^{-4}$	–	–
4	-1.4608542	–	–
5	1.1732398	–	–
6	6.47293618×10^{3}	–	–
mid-latitude cluster			
i	$a_{\mathrm{NO_x,m,i}}$	$a_{\mathrm{H_2O,m,i}}$	$a_{\mathrm{CiC,m,i}}$
0	$4.78782759 \times 10^{-4}$	$1.11758077 \times 10^{-12}$	$2.56886171 \times 10^{-21}$
1	1.28634039×10^{2}	1.4423854×10^{-3}	$-5.84017454 \times 10^{-17}$
2	$5.2802694 \times 10^{-14}$	$5.91431647 \times 10^{-3}$	$-3.02860089 \times 10^{-14}$
3	$-7.52058168 \times 10^{-4}$	4.86022794	$-1.36665996 \times 10^{-3}$
4	–	–	$-1.17906742 \times 10^{-2}$
5	–	–	5.452753
6	–	–	5.03288373×10^{1}
7	–	–	-7.7344541×10^{3}
tropical cluster			
i	$a_{\mathrm{NO_x,t,i}}$	$a_{\mathrm{H_2O,t,i}}$	$a_{\mathrm{CiC,t,i}}$
0	$1.41434794 \times 10^{-1}$	$1.04883173 \times 10^{-8}$	$3.58811246 \times 10^{-5}$
1	$1.15507399 \times 10^{-3}$	$1.35263527 \times 10^{-3}$	2.18840126×10^{1}
2	4.9301452×10^{-2}	$7.62155078 \times 10^{-7}$	$-1.91139484 \times 10^{-13}$
3	$6.06235609 \times 10^{-12}$	$2.94922714 \times 10^{-4}$	$-5.63576858 \times 10^{-5}$
4	$-2.90148707 \times 10^{-10}$	–	$5.92278899 \times 10^{-7}$
5	$5.02677523 \times 10^{-8}$	–	$-1.63789849 \times 10^{-3}$
6	–	–	1.13661959

The derived $\mathrm{EI(NO_x)}$ regression formulas vary for distances smaller and larger than 2000 km and are described by

$$\mathrm{EI(NO_x)} = \begin{cases} a_0 + a_1 \ln \dfrac{d}{\mathrm{km}} & \text{if } d < 2000\,\mathrm{km} \\ a_2 + a_3 d + a_4 d^2 + a_5 d^3 & \text{if } d \geq 2000\,\mathrm{km}\,. \end{cases} \tag{8}$$

https://doi.org/10.5194/gmd-2023-126
Preprint. Discussion started: 27 June 2023

Geoscientific Model Development Discussions
Open Access
EGU

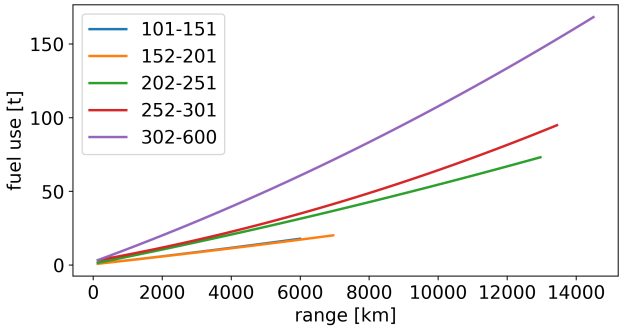

Figure 6. Fuel functions for the simplified calculation of burnt fuel as a function of flight distance.

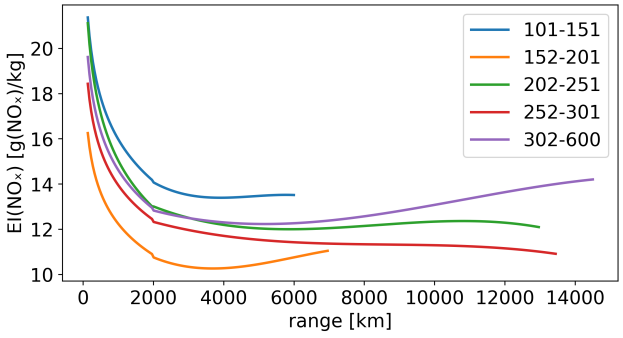

Figure 7. NO_x functions for the simplified calculation of the NO_x emission index as a function of flight distance.

Best fit solutions for $EI(NO_x)$ regression formulas are provided in Tables 3 and 4 and Fig. 7. The fuel and NO_x functions are not used for the derivation of the climate effect regression formulas, where the exact values for each flight are used. Nonetheless, we provide them as additional information that might be useful and can be applied in the simplified estimation of a flight's climate effect, as only the seat category and the flight distance are required for their computation.

An interesting feature of the NO_x functions (Eq. 8; Fig. 7) is the lack of correlation between the seat category and the $EINO_x$. The $EINO_x$ mainly depends on the combustion temperature, with a higher temperature leading to more emissions. The combustion temperature depends on the properties of the engine in the specific aircraft. For the computation of the NO_x functions, aircraft that are frequently used within their seat category were chosen, but these are not necessarily representative of the entirety of used aircraft within that seat category. In particular, the most efficient and therefore economically successful aircraft may be overrepresented.

https://doi.org/10.5194/gmd-2023-126
Preprint. Discussion started: 27 June 2023

Geoscientific Model Development Discussions

Table 2. Best fit solutions for fuel regression formulas.

Seat category	maximum range [km]	a_0 [kg]	a_1 [kgkm^{-1}]	a_2 [kgkm^{-2}]	R^2
101-151	6,000	632.36	2.5809	5.0×10^{-5}	0.9997
152-201	7,000	629.27	2.5388	3.8×10^{-5}	0.9992
202-251	13,000	997.62	4.6586	7.3×10^{-5}	0.9994
252-301	13,450	2,789.10	4.1618	2.2×10^{-4}	0.9907
302-600	14,500	2,277.30	8.5406	2.4×10^{-4}	0.9999

Table 3. Best fit solutions for EI(NO_x) regression formulas for flight distances < 2000km.

Seat category	a_0 [g(NO_2)kg^{-1}]	a_1 [g(NO_2)kg^{-1}]	R^2
101-151	34.403	-2.667	0.868
152-201	25.963	-1.986	0.892
202-251	35.811	-3.007	0.923
252-301	29.287	-2.220	0.930
302-600	31.717	-2.475	0.971

3 Results and discussion

The climate effect functions can generally capture the trend, as can be seen by the fits (gray dots in Fig. 3-5) and by the mean absolute relative error of the fit, which we define as

$$\mathrm{MARE} = \frac{1}{N} \sum_{i=1}^{N} \left| \frac{\mathrm{ATR100}_{\mathrm{tot}}^{\mathrm{true}} - \mathrm{ATR100}_{\mathrm{tot}}^{\mathrm{fit}}}{\mathrm{ATR100}_{\mathrm{tot}}^{\mathrm{true}}} \right|, \tag{9}$$

where N is the number of flights. The MARE is 9.4 % for the short-flight cluster, 16.1 % for the mid-latitude cluster, and 15.0 % for the tropical cluster. When combining results from the different clusters, this leads to $\mathrm{MARE} = 15.0\%$ and a root mean square error of 1.24 nK. The true model values obtained by AirClim are generally strongly correlated with the values obtained from the climate effect functions (Fig. 8). However, the features of the correlation between true model values and fit values differ for each climate effect contribution. For NO_x, there is very good correlation at short flight distances, but the fits fail to mirror the large variability at long distances ($>\sim 5000$km) and instead predict a more confined behavior. For H_2O, some rather short flights ($\sim 500 - 1000$km) are overestimated by the fits. For the climate effect through contrails, flights with a low climate effect per distance travelled may be both overestimated or underestimated, but the correlation is better at higher climate effects. The correlation of the total climate effect is better than that of the individual contributions, owing partly to the addition of CO_2 climate effects, which are linear in the model and therefore perfectly fit.

Since the climate effect functions for the different clusters are independent of each other, mismatches at the cluster boundaries cannot be avoided (Fig. 9 - 10). The lines in Fig. 9 - 10 indicate the climate effect at the cluster boundary calculated

https://doi.org/10.5194/gmd-2023-126
Preprint. Discussion started: 27 June 2023

Geoscientific Model Development Discussions

Table 4. Best fit solutions for $\mathrm{EI(NO_x)}$ regression formulas for flight distances $\geq 2000\mathrm{km}$.

Seat category	a_2 $[\mathrm{g(NO_2)kg^{-1}}]$	a_3 $[\mathrm{g(NO_2)kg^{-1}km^{-1}}]$	a_4 $[\mathrm{g(NO_2)kg^{-1}km^{-2}}]$	a_5 $[\mathrm{g(NO_2)kg^{-1}km^{-3}}]$	R^2
101-151	17.478	-2.70×10^{-3}	5.8×10^{-7}	-4×10^{-11}	0.978
152-201	13.163	-1.84×10^{-3}	3.6×10^{-7}	-2×10^{-11}	0.992
202-251	14.742	-1.14×10^{-3}	1.5×10^{-7}	-6×10^{-12}	0.970
252-301	13.428	-6.93×10^{-4}	7.8×10^{-8}	-3×10^{-12}	0.970
302-600	13.992	-7.61×10^{-4}	9.7×10^{-8}	-3×10^{-12}	0.970

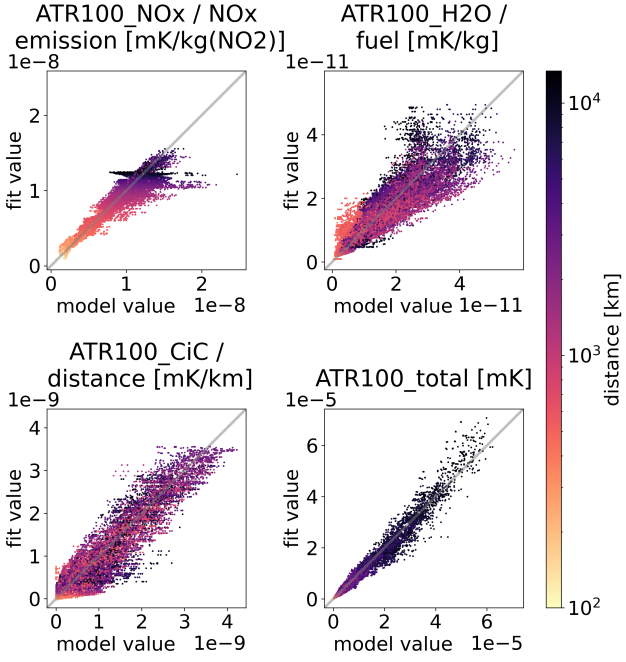

Figure 8. Correlation plots contrasting the true model values of quantities $\mathrm{ATR100_{NO_x}}/e$, $\mathrm{ATR100_{H_2O}}/f$, $\mathrm{ATR100_{CiC}}/d$, and $\mathrm{ATR100_{tot}}$ obtained by AirClim with the fit values obtained from the climate effect functions. The color indicates flight distance. The gray line is the 1:1 line.

using the equations for either cluster for a flight with average $\mathrm{NO_x}$ emissions and fuel use. The difference between lines of the same color indicates the mismatch. For average $\mathrm{NO_x}$ emissions and fuel use cases, the mismatch is never larger than 83%. Particularly large mismatches are found between the short-flight and the tropical cluster for flights with a mean latitude in the equatorial region (Fig. 10), as well as for very long flights between the mid-latitude and tropical clusters (Fig. 9). We also calculated the climate effect at the cluster boundary using either cluster for flights with minimal and maximal $\mathrm{NO_x}$ emissions and for flights with minimal and maximal fuel use and found that the most extreme mismatch, reaching 128%, is between cal-

https://doi.org/10.5194/gmd-2023-126
Preprint. Discussion started: 27 June 2023

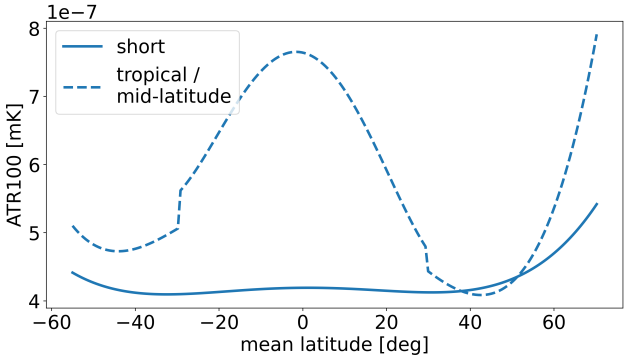

Figure 9. ATR100 at the cluster boundary of 462 km computed from different clusters' climate effect functions for average NO_x emissions and fuel use. Average conditions are taken as the average of all flights with flight distances of 462 ± 50km.

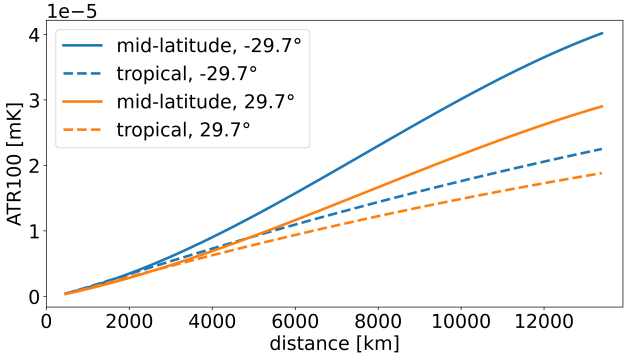

Figure 10. ATR100 at the cluster boundaries of 29.7°N (blue) and 29.7°S (orange) computed from different clusters' climate effect functions. The average fuel use per flight distance and NO_x emissions per flight distance of all flights with mean latitudes of 29.7 ± 2°N and 29.7 ± 2°S, respectively, were used in the computation.

culations using the climate effect functions for the tropical and mid-latitude cluster for a flight with maximal NO_x emissions at very long flight distances with a mean latitude of 29.7°S.

Table 5 shows the climate effect components of selected example flights, representing the three clusters and different seat categories. The values in the table are computed for a distance that is 95 km larger than the great circle distance to account for arrival and departure procedures according to the EN 16258 standard. The relation between non-CO_2 effects and CO_2 is higher than the factor of 2 to 3 known from the literature for non-CO_2 effects of aviation, which is based on the total CO_2 level from pre-industrial times (e.g., from 1940 to 2018 for Lee et al., 2021). The level of the $CO_{2,e}$ factors strongly depends on the level of the CO_2 reference. Since $CO_{2,e}$ climate effect functions are designed to estimate the climate impact of present and future flights, we do not consider any emissions of historic aviation. As the climate impact of CO_2 is more affected by the historical emission than short lived non-CO_2 effects, this leads to larger $CO_{2,e}$ factors in this study. Another reason for the

https://doi.org/10.5194/gmd-2023-126
Preprint. Discussion started: 27 June 2023

Geoscientific Model Development Discussions

Table 5. Climate effects and $CO_{2,e}$ factors for selected example flights.

Seat category	101-151	152-201	252-301
Origin airport	LHR	JFK	MAD
Destination airport	CDG	MUC	BUE
Distance[a] [km]	443	6572	10147
Mean latitude [°N]	50.25	49.89	3.20
Fuel burn[b] [kg]	1784	18971	68910
NO_x emission[c] [kg]	32.4	190.2	788.5
Cluster	short-flight	mid-latitude	tropical
$ATR100_{CO_2}$ [nK]	1.44	15.32	55.66
$ATR100_{H_2O}$ [nK]	0.02	6.03	3.25
$ATR100_{NO_x}$ [nK]	1.14	22.28	100.22
$ATR100_{CiC}$ [nK]	0.73	31.27	242.49
$ATR100_{tot}$ [nK]	3.33	74.91	401.62
$CO_{2,e}$ factor	2.3	4.9	7.2

[a] Great circle distance + 95 km; [b] according to Eq. 7; [c] according to Eq. 8

larger $CO_{2,e}$ factors in this study is that previous studies sometimes only included line-shaped contrails, but no contrail cirrus (e.g.; IPCC, 1999; Sausen et al., 2005).

4 Summary and conclusions

Within this study, we developed a method for a simplified estimate of CO_2 equivalents per flight. The simplified calculation method aims at estimating non-CO_2 climate effects of air traffic as precisely as possible, without detailed information on the actual flight route, actual fuel burn, and the current weather situation. For this purpose, we evaluated a data set containing a global set of detailed flight trajectories, flight emissions, and climate responses for various aircraft types with seat capacities ranging from 101 to 600. Based on that data set, we generated climate effect functions and regression formulas for fuel consumption and NO_x emissions.

In order to increase the accuracy of the climate effect functions, flights were clustered using the K-Means clustering algorithm. The resulting three clusters have distinct characteristics. For flights in the short-flight cluster, the contribution of contrails to the climate effect is very low at an average of 3.5% of the total climate effect, whereas the contribution of CO_2 is strong at an average of 57.4% of the total climate effect. Flights in this cluster often do not reach sufficient altitudes for contrail formation. The climate effect of the tropical cluster is dominated by contrails (average contribution of 56.6%) because contrails have a particularly large climate effect in the tropics. The mid-latitude cluster contains the remaining flights and has large climate effect contributions from NO_x and H_2O (average contributions of 49.1% and 6.8%, respectively).

https://doi.org/10.5194/gmd-2023-126
Preprint. Discussion started: 27 June 2023


Geoscientific Model Development Discussions
Open Access
EGU

The resulting climate effect functions (Eq. 2-5) can be used in combination with their best-fit coefficients (Table 1) to efficiently compute the climate effect in terms of ATR100 of any flight with given distance, mean latitude, fuel use, and NO_x emissions without the need to run a climate response model.

By deriving climate effect functions for each of the simplified clusters, the mean absolute relative error of all flights and aircraft types was reduced to 15.0%, which represents the AirClim computations 5% better than the $CO_{2,e}$ regression formulas of Dahlmann et al. (2023) for the A330-200 aircraft. The mean absolute relative error is 9.4% for the short-flight cluster, 16.1% for the mid-latitude cluster, and 15.0% for the tropical cluster. Since the climate effect functions for the different clusters are independent from each other, mismatches at the cluster boundaries cannot be avoided. For average NO_x emissions and fuel use cases, the mismatch is never larger than a factor of two. Particularly large mismatches are found between the short-flight and the tropical cluster for flights with a mean latitude in the equatorial region, as well as for very long flights between the mid-latitude and tropical clusters.

The climate effect functions and the regression formulas for fuel and $EI(NO_x)$ that were derived in this study were also embedded into an Excel application called "simplified CO_2 equivalent estimator", which we provide in the supplementary materials. After a selection of input values (climate metric; aircraft seat category; origin and destination airports; flight frequency), the tool returns

- the great circle distance (GCD) plus 95 km for arrival and departure procedures,
- a fuel burn estimate,
- estimated CO_2 and NO_x emissions, and
- CO_2 equivalents for H_2O, NO_x, and CiC.

This simplified estimate of CO_2 equivalents is designed for climate footprint assessments, for which the climate effect functions provide a more accurate representation than constant factors for non-CO_2 effects. The tool is not designed for use in an emissions trading system because this would require the actual flight routes and profiles to reflect mitigation measures such as lower flight altitudes or the avoidance of regions with large contrail climate effects, which are not included when assuming standard flight profiles and great circle routes. However, the tool allows for providing an estimate for plausibility checks or a backup when airlines are unable to provide the more detailed data.

Code availability. The python code used for the clustering and generation of the climate effect functions as well as the creation of the figures is given in Thor et al. (2023).

https://doi.org/10.5194/gmd-2023-126
Preprint. Discussion started: 27 June 2023

Geoscientific Model Development Discussions
Open Access
EGU

Appendix A: User guide

For simplifying the estimation of CO_2 equivalents per flight, the resulting climate effect functions and regression formulas for fuel and NO_x were embedded into an Excel application. The basic user version of the Excel application consists of three Excel sheets: “Info”, “Calculator”, and “AirportDatabase”:

1. The “Info” sheet provides general information such as the release date and the version number. In addition, you will find an instruction for the use of DLR’s simplified CO_2 equivalent estimator and an exclusion of liability.

2. The “Calculator” sheet is the core of the application. All input values are entered in this sheet and all calculation results are displayed.

3. The “AirportDatabase” provides detailed position information for almost 9000 airports. Airports are identified via the IATA airport code, which is a three-letter geocode defined by the International Air Transport Association (IATA). If the desired airports are not included in the "AirportDatabase" sheet, users are free to add them.

In the developer version of the Excel application there are two more Excel sheets: Fuel & NO_x functions and “$CO_{2,e}$ functions”

1. In the “Fuel & NO_x functions” sheet, regression formulas, and polynomial coefficients are stored for various aircraft classes. These formulas and coefficients are used for the calculation of the fuel consumption and the cruise emission index of nitrogen oxides.

2. The “$CO_{2,e}$ functions” sheet provides all necessary formulas and polynomial coefficients for the climate effect function calculation. Formulas and coefficients are stored separately for the “short-flight”, “mid-latitude”, and “tropical” cluster and differ according to the climate agent (CO_2, H_2O, NO_x, CiC). In addition, conversion factors are stored here, which allow to express the $CO_{2,e}$ either in the climate metric ATR100 or in AGWP100 (absolute global warming potential over 100 years).

The calculations of CO_2 equivalents is based on following input parameters, which users enter into the "Calculator" spreadsheet of the Excel application:

1. Selection of the preferred climate metric for the calculation of CO_2 equivalents in cell "B2". The drop-down list allows the user to choose between ATR100 or AGWP100.

2. Selection of the preferred aircraft seat category in column “A”. A drop-down list allows the user to choose between five different seat categories. The proposed seat categories range from 101-151 seats to 302-600 seats and represent following aircraft types:

   - 101-151 seats: like Airbus A319, A320, Boeing 737
   - 152-201 seats: like Airbus A320, A321, Boeing 737, 757
   - 202-251 seats: like Airbus A330, A340, Boeing 767, 777

https://doi.org/10.5194/gmd-2023-126
Preprint. Discussion started: 27 June 2023

Geoscientific Model Development Discussions

- 252-301 seats: like Airbus A330, Boeing 777
- 302-600 seats: like Airbus A340, A380, Boeing 747, 777

3. Enter the IATA airport code of the origin and destination airports in columns “B” and “C”. Columns “E” and “F” indicate whether the airports are included in the "AirportDatabase" sheet or not. If one of the desired airports is not included, users are free to add it in the "AirportDatabase" sheet. Also indicated in the "G" column of the "Calculator" sheet is whether the selected origin–destination pair is flyable with the selected aircraft seat category.
4. The number of flights performed on the city pair connection is entered into column “D”. The value "1" is the minimum input value here.
5. Output parameters

If all entries have been made correctly the “Simplified $CO_{2,e}$ Estimator” will return the following output data in columns “H” to “T” of the “Calculator” sheet:

- The great circle distance (GCD) plus 95km for arrival and departure procedures (in km),
- The fuel burn estimate (in kg),
- The estimated amount of CO_2 emissions (in kg),
- The estimated amount of NO_x emissions (in kg),
- The estimated CO_2 equivalents of H_2O, NO_x, and CiC (in kg), based on ATR100 and AGWP100
- The estimated CO_2 equivalents of all non-CO_2 effects (in kg),
- The estimated CO_2 equivalents of all effects (CO_2 and non-CO_2 effects) (in kg),
- The estimated CO_2 equivalent factor of the flight (CO_2 equivalents / CO_2).

In row 2 of the “Calculator” sheet, aggregated values for all flights are displayed for the distance, fuel consumption, emissions (CO_2, NO_x), and CO_2 equivalents (total value, value of all non-CO_2 effects, mean factor).

Author contributions. R. N. T. performed the clustering, the regressions for the climate effect functions, created all figures, and wrote the manuscript with the help of all coauthors. F. L. simulated the trajectories and created the emissions inventory. K. D. computed the aviation climate effects using AirClim. M. N. created the regressions for fuel use and NO_x emissions and the Excel tool. V. G., S. M. and F. L. conceptualized the research.

Competing interests. Volker Grewe is a member of the editorial board of the journal.

https://doi.org/10.5194/gmd-2023-126
Preprint. Discussion started: 27 June 2023

Acknowledgements. This work is part of the project „Untersuchung der praktischen Umsetzung der Einbringung von Nicht-CO_2-Treibhausgas-Effekten im Luftverkehr in das EU-ETS einschließlich Clusteranalyse“, funded by the German Environment Agency (Umweltbundesamt – UBA). The authors thank S. Zechlau for a through internal review.

https://doi.org/10.5194/gmd-2023-126
Preprint. Discussion started: 27 June 2023

Geoscientific Model Development Discussions

References

Brazzola, N., Patt, A., and Wohland, J.: Definitions and implications of climate-neutral aviation, Nature Climate Change, 12, 761–767, https://doi.org/10.1038/s41558-022-01404-7, 2022.

Burkhardt, U. and Kärcher, B.: Global radiative forcing from contrail cirrus, Nature Clim. Change, 1, 54–58, https://doi.org/10.1038/nclimate1068, 2011.

Cames, M., Graichen, J., Siemons, A., and Cook, V.: Emission reduction targets for international aviation and shipping, Tech. Rep. IP/A/ENVI/2015-11, Policy Department A for the Committee on Environment, Public Health and Food Safety (ENVI), 2015.

Dahlmann, K., Grewe, V., Frömming, C., and Burkhardt, U.: Can we reliably assess climate mitigation options for air traffic scenarios despite large uncertainties in atmospheric processes?, Transportation Research Part D: Transport and Environment, 46, 40–55, https://doi.org/10.1016/j.trd.2016.03.006, 2016a.

Dahlmann, K., Koch, A., Linke, F., Lührs, B., Grewe, V., Otten, T., Seider, D., Gollnick, V., and Schumann, U.: Climate-Compatible Air Transport System – Climate Impact Mitigation Potential for Actual and Future Aircraft, Aerospace, 3, 38, https://doi.org/10.3390/aerospace3040038, 2016b.

Dahlmann, K., Grewe, V., Matthes, S., and Yamashita, H.: Climate assessment of single flights: Deduction of route specific equivalent CO_2 emissions, International Journal of Sustainable Transportation, 17, 29–40, https://doi.org/10.1080/15568318.2021.1979136, 2023.

Dray, L., Schäfer, A. W., Grobler, C., Falter, C., Allroggen, F., Stettler, M. E., and Barrett, S. R.: Cost and emissions pathways towards net-zero climate impacts in aviation, Nature Climate Change, 12, 956–962, https://doi.org/10.1038/s41558-022-01485-4, 2022.

Dube, K.: Emerging from the COVID-19 Pandemic: Aviation Recovery, Challenges and Opportunities, Aerospace, 10, 19, https://doi.org/10.3390/aerospace10010019, 2023.

DuBois, D. and Paynter, G. C.: "Fuel Flow Method 2" for Estimating Aircraft Emissions, SAE Transactions, 115, 1–14, https://doi.org/10.2307/44657657, 2006.

Faber, J., Greenwood, D., Lee, D., Mann, M., de Leon, P. M., Nelissen, D., Owen, B., Ralph, M., Tilston, J., van Velzen, A., and van de Vreede, G.: Lower NO_x at higher altitudes policies to reduce the climate impact of aviation NO_x emission, Tech. Rep. 08.7536.32, CE Delft, 2008.

Fichter, C.: Climate Impact of Air Traffic Emissions in Dependency of the Emission Location, Ph.D. thesis, Manchester Metropolitan University, Manchester, UK, 2009.

Forster, P. M. d. F., Shine, K. P., and Stuber, N.: It is premature to include non-CO2 effects of aviation in emission trading schemes, Atmospheric Environment, 40, 1117–1121, https://doi.org/10.1016/j.atmosenv.2005.11.005, 2006.

Ghosh, R., Wicke, K., Kölker, K., Terekhov, I., Linke, F., Niklaß, M., Lührs, B., and Grewe, V.: An Integrated Modelling Approach for Climate Impact Assessments in the Future Air Transportation System–Findings from the WeCare Project, in: 2nd ECATS Conference 2016, 2016.

Grewe, V. and Stenke, A.: AirClim: an efficient tool for climate evaluation of aircraft technology, Atmospheric Chemistry and Physics, 8, 4621–4639, https://doi.org/10.5194/acp-8-4621-2008, 2008.

Grewe, V., Dahlmann, K., Flink, J., Frömming, C., Ghosh, R., Gierens, K., Heller, R., Hendricks, J., Jöckel, P., Kaufmann, S., Kölker, K., Linke, F., Luchkova, T., Lührs, B., Van Manen, J., Matthes, S., Minikin, A., Niklaß, M., Plohr, M., Righi, M., Rosanka, S., Schmitt, A., Schumann, U., Terekhov, I., Unterstrasser, S., Vázquez-Navarro, M., Voigt, C., Wicke, K., Yamashita, H., Zahn, A., and

https://doi.org/10.5194/gmd-2023-126
Preprint. Discussion started: 27 June 2023

Ziereis, H.: Mitigating the climate impact from aviation: Achievements and results of the DLR WeCare project, Aerospace, 4, 34, https://doi.org/10.3390/aerospace4030034, 2017a.

Grewe, V., Matthes, S., Frömming, C., Brinkop, S., Jöckel, P., Gierens, K., Champougny, T., Fuglestvedt, J., Haslerud, A., Irvine, E., and Shine, K.: Feasibility of climate-optimized air traffic routing for trans-Atlantic flights, Environmental Research Letters, 12, 034 003, https://doi.org/10.1088/1748-9326/aa5ba0, 2017b.

Grewe, V., Gangoli Rao, A., Grönstedt, T., Xisto, C., Linke, F., Melkert, J., Middel, J., Ohlenforst, B., Blakey, S., Christie, S., Matthes, S., and Dahlmann, K.: Evaluating the climate impact of aviation emission scenarios towards the Paris agreement including COVID-19 effects, Nature Communications, 12, 3841, https://doi.org/10.1038/s41467-021-24091-y, 2021.

ICAO: Annual Report of the ICAO Council: 2015, https://www.icao.int/annual-report-2015/Documents/Appendix_1_en.pdf, accessed: 2023-02-22, 2015.

ICAO: Annual Report of the ICAO Council: 2021, https://www.icao.int/annual-report-2021/Documents/ARC_2021_Air%20Transport%20Statistics_final_sched.pdf, accessed: 2023-02-22, 2021.

IEA: Aviation, https://www.iea.org/reports/aviation, accessed: 2023-05-17, 2022.

IPCC: The Supplementary Report to the IPCC Scientific Assessment, in: Climate Change 1992, edited by Houghton, J. T., Callander, B. A., and Varney, S. K., WMO/UNEP, Cambridge University Press, Cambridge, UK, 200 pp., 1992.

IPCC: Aviation and the global atmosphere, in: A Special Report of the Intergovernmental Panel on Climate Change, edited by Penner, J. E., Lister, D., Griggs, D. J., Dokken, D. J., and McFarland, M., Cambridge University Press, 1999.

Kärcher, B.: Formation and radiative forcing of contrail cirrus, Nature Communications, 9, 1824, https://doi.org/10.1038/s41467-018-04068-0, 2018.

Köhler, M., Rädel, G., Shine, K., Rogers, H., and Pyle, J.: Latitudinal variation of the effect of aviation NO_x emissions on atmospheric ozone and methane and related climate metrics, Atmospheric Environment, 64, 1–9, https://doi.org/10.1016/j.atmosenv.2012.09.013, 2013.

Lee, D., Fahey, D., Skowron, A., Allen, M., Burkhardt, U., Chen, Q., Doherty, S., Freeman, S., Forster, P., Fuglestvedt, J., Gettelman, A., De León, R., Lim, L., Lund, M., Millar, R., Owen, B., Penner, J., Pitari, G., Prather, M., Sausen, R., and Wilcox, L.: The contribution of global aviation to anthropogenic climate forcing for 2000 to 2018, Atmospheric Environment, 244, 117 834, https://doi.org/10.1016/j.atmosenv.2020.117834, 2021.

Linke, F.: Environmental Analysis of Operational Air Transportation Concepts, Ph.D. thesis, Hamburg University of Technology, 2016.

Lührs, B., Linke, F., and Gollnick, V.: Erweiterung eines Trajektorienrechners zur Nutzung meteorologischer Daten für die Optimierung von Flugzeugtrajektorien, in: 63. Deutscher Luft- und Raumfahrtkongress 2014 (DLRK), 2014.

Matthes, S., Lim, L., Burkhardt, U., Dahlmann, K., Dietmüller, S., Grewe, V., Haslerud, A. S., Hendricks, J., Owen, B., Pitari, G., Righi, M., and Skowron, A.: Mitigation of non-CO_2 aviation's climate impact by changing cruise altitudes, Aerospace, 8, 36, https://doi.org/10.3390/aerospace8020036, 2021.

Meinshausen, M., Smith, S. J., Calvin, K., Daniel, J. S., Kainuma, M. L. T., Lamarque, J.-F., Matsumoto, K., Montzka, S. A., Raper, S. C. B., Riahi, K., Thomson, A., Velders, G. J. M., and van Vuuren, D. P. P.: The RCP greenhouse gas concentrations and their extensions from 1765 to 2300, Climatic Change, 109, 213–241, https://doi.org/10.1007/s10584-011-0156-z, 2011.

Niklaß, M., Dahlmann, K., Grewe, V., Maertens, S., Plohr, M., Scheelhaase, J., Schwieger, J., Brodmann, U., Kurzböck, C., Schweizer, N., and von Unger, M.: Integration of Non-CO_2 Effects of Aviation in the EU ETS and under CORSIA, Tech. Rep. (UBA-FB) FB000270/ENG, German Environment Agency, 2019a.

https://doi.org/10.5194/gmd-2023-126
Preprint. Discussion started: 27 June 2023

Niklaß, M., Lührs, B., Grewe, V., Dahlmann, K., Luchkova, T., Linke, F., and Gollnick, V.: Potential to reduce the climate impact of aviation by climate restricted airspaces, Transport Policy, 83, 102–110, https://doi.org/10.1016/j.tranpol.2016.12.010, 2019b.

Pedregosa, F., Varoquaux, G., Gramfort, A., Michel, V., Thirion, B., Grisel, O., Blondel, M., Prettenhofer, P., Weiss, R., Dubourg, V., Vanderplas, J., Passos, A., Cournapeau, D., Brucher, M., Perrot, M., and Duchesnay, E.: Scikit-learn: Machine Learning in Python, Journal of Machine Learning Research, 12, 2825–2830, 2011.

Sausen, R., Isaksen, I., Grewe, V., Hauglustaine, D., Lee, D. S., Myhre, G., Köhler, M. O., Pitari, G., Schumann, U., Stordal, F., and Zerefos, C.: Aviation radiative forcing in 2000: An update on IPCC (1999), Meteorologische Zeitschrift, 14, 555–561, https://doi.org/10.1127/0941-2948/2005/0049, 2005.

Scheelhaase, J. D., Dahlmann, K., Jung, M., Keimel, H., Nieße, H., Sausen, R., Schaefer, M., and Wolters, F.: How to best address aviation's full climate impact from an economic policy point of view? – Main results from AviClim research project, Transportation Research Part D: Transport and Environment, 45, 112–125, https://doi.org/10.1016/j.trd.2015.09.002, 2016.

Thor, R. N., Niklaß, M., Dahlmann, K., Linke, F., Grewe, V., and Matthes, S.: Code used in "The CO2 and non-CO2 climate effects of individual flights: simplified estimation of CO2 equivalents" (Thor et al., GMD, 2023), Zenodo, https://doi.org/10.5281/zenodo.8038803, 2023.

Voigt, C., Kleine, J., Sauer, D., Moore, R. H., Bräuer, T., Clercq, P. L., Kaufmann, S., Scheibe, M., Jurkat-Witschas, T., Aigner, M., Bauder, U., Boose, Y., Borrmann, S., Crosbie, E., Diskin, G. S., DiGangi, J., Hahn, V., Heckl, C., Huber, F., Nowak, J. B., Rapp, M., Rauch, B., Robinson, C., Schripp, T., Shook, M., Winstead, E., Ziemba, L., Schlager, H., and Anderson, B. E.: Cleaner burning aviation fuels can reduce contrail cloudiness, Commun Earth Environ, 2, https://doi.org/10.1038/s43247-021-00174-y, 2021.